



INTERNATIONAL ATOMIC ENERGY AGENCY
UNITED NATIONS EDUCATIONAL, SCIENTIFIC AND CULTURAL ORGANIZATION



INTERNATIONAL CENTRE FOR THEORETICAL PHYSICS
34100 TRIESTE (ITALY) - P.O.B. 586 - MIRAMARE - STRADA COSTIERA 11 - TELEPHONES: 224241/233420
CABLE: CENTRATOM - TELEX 460392-1

SMR/93 - 38

AUTUMN COURSE ON GEOMAGNETISM, THE IONOSPHERE
AND MAGNETOSPHERE

(21 September - 12 November 1982)

RAY TRACING STUDIES OF WHISTLER GUIDANCE

M. DOBROWOLNY
Istituto Fisica Spazio
Interplanetario
C.N.R.
C.P. 27
00044 Frascati (Roma)
Italy

These are preliminary lecture notes, intended only for distribution to participants.
Missing or extra copies are available from Room 230.



6. RAY TRACING STUDIES OF WHISTLER GUIDANCE

6.1 Refractive index surfaces for whistler waves

Let us briefly recall what are the features of the refractive index surfaces for whistler waves. The index of refraction is given by (see Sect. 2)

$$n(\theta) = \frac{\omega_{pe} / |\omega_{ac}|}{\Lambda^{1/2} (\omega_{pe}^2 - \Lambda)^{1/2}} \quad (6.1)$$

where $\Lambda = \omega / |\omega_{Be}|$. This formula holds when $\omega_{pe}^2 \gg \omega_{Be}^2$ and for $\omega < |\omega_{Be}|$. Note that the magnitude of the refractive index is proportional to the square root of the electron density.

The general shapes of the cross sections of the refractive index surfaces computed from eq. (6.1) are shown in Fig. 18. The curve (a) shows the limiting shape when $\Lambda \rightarrow 0$ (and corresponds to the simplified formula of Eckersley and Storey). It is seen there that the ray direction is parallel to the magnetic field only for $\theta = 0$. Curve (b) refers to the range $0 < \Lambda < 0.5$ where things become more complicated. There is then a limiting cone angle θ_L given by

$$\theta_L = \arccos \Lambda \quad (6.2)$$

such that, for $\theta > \theta_L$, $n(\theta)$ becomes imaginary and propagation is no more possible. Now we have a maximum of the refractive surface (at $\theta = 0$) and two minima at $\theta = \pm \theta_2$ with

$$\theta_2 = \arccos 2\Lambda \quad (6.3)$$

Correspondingly, the ray direction is parallel to the magnetic field

both at $\theta = 0$ and at $\theta = \pm \theta_2$. Finally, curve (c) gives the shape of the surface when $0.5 < \Lambda < 1$. There is, again, a limiting cone angle for propagation given by θ_L and now (like for $\Lambda \rightarrow 0$) the ray direction is parallel to the magnetic field only for $\theta = 0$.

6.2 Whistlers ray paths in slowly inhomogeneous ionospheres and magnetospheres

Calculations of whistler ray paths, using either one of the methods outlined in Sect. 5, were done by different authors for various initial conditions and various smooth ionospheric models. For example Yabroff (1959, 1961) finds that the ray path depends from the initial wave normal angle and that the final wave normal angle is in general very different from the initial value. Taking a first hop whistler with a wave normal approximately along the vertical, the normal at the other hand of the path was found to approach 90° with respect to the magnetic field direction. It is from this value of final wave normal of the first hop whistler that the initial value of wave normal of the reflected second hop whistler has to be calculated. The result is that, in such cases, the second hop whistler is found to be away from the vertical and, contrary to the observation of echoes, the ray path of the second whistler could not be the same as that of the first.

The general conclusion, from these and other related works is that reasonable smooth variations of the ionospheric parameters were found to be insufficient to explain the whistler's guiding indicated by the observations. To explain several observational features (Smith, 1961; Helliwell, 1965), one needs a duct within which the energy of the whistler's signal remains trapped during propagation. It was proposed, in the early work of Smith et al. (1960) referred to whistlers, and in successive work by Booker (1962), that such a ducting action could

be accomplished by the presence of field aligned irregularities of ionization extending between the hemispheres.

6.3 Ray theory of trapping of whistlers in field aligned ducts

6.3.1 Cases $A \sim 0$ and $0.5 < A < 1$

For simplicity we will assume that the static magnetic field is constant in magnitude and direction (which we take as the x axis). We also suppose to have an electron density varying in the direction H_0 (the y direction). The density profiles, along y, are shown on the right of Fig. 30a and b where we suppose to have, respectively, a density crest or a density through, centered along a given magnetic field line.

We will now show, using the graphical construction of ray theory (see Sect. 5) that, due to the fact that $n(\theta) = n_0^{1/2}$, these density variations can produce focusing of the whistler rays and eventually confinement of whistler's energy parallel to the magnetic field direction.

Fig. 30a indicates how this occurs for the case $A \sim 0$. The left hand part contains three refractive index surfaces (of the general shape of Fig. 18a), which corresponds to different lateral displacements (in y) of the ray (and are different because of the density inhomogeneity which is taken, in this case, as a crest). More precisely, μ_0 denotes the refractive index surface corresponding to the axis ($y=0$) of the density inhomogeneity; μ_2 is the surface corresponding to what will be seen to be the maximum lateral displacement of a given ray (value $N(P)$ on the density profile on the right); μ_1 corresponds to an intermediate displacement, as can be seen from the right hand part of Fig. 30a. We suppose the initial wave normal to be in the x-y plane at

an angle θ_0 with respect to the magnetic field. The corresponding initial ray direction is indicated with R_0 . This direction implies an initial lateral displacement of the ray in the y-direction. For a displacement to a density value corresponding to the value μ_1 of refractive index, we construct the new ray direction in the way explained in Sect. 5.2 namely: we draw the parallel to the gradient direction (y) from the point, on the μ_0 surface, where R_0 is drawn; find the intersection of this line with the μ_1 surface; the normal to μ_1 there gives the new ray direction R_1 at the lateral displacement considered. Clearly, this second ray direction, like the new wave normal, is less inclined, with respect to H_0 , than the initial ray R_0 . Now, the parallel to y from the tip of the refractive index vector at μ_1 , becomes tangent at $\theta=0$ to a refractive index surface, denoted with μ_2 , corresponding to a certain density value $N(P)$ and, hence, to a certain lateral displacement of the ray. There, by construction, the new wave normal and ray direction (R_2) are both parallel to the magnetic field so that focusing of the initial ray considered (R_0) has been accomplished. From the symmetry of the construction based on Snell's law, it is clear that the upper half of the ray path (after maximum lateral excursion) is the mirror image of the lower half with respect to a horizontal line through the maximum lateral excursion, as it is indicated on the right of the figure. Here R_4 denote the ray direction when the ray reaches again the density maximum. Then the same pattern is repeated again on the opposite side of the density irregularity. The final shape of the ray path in the case considered ($A \sim 0$ and a density crest) is that denoted by curve (a) in Fig. 31.

Exactly the same considerations can be repeated on Fig. 30b which refers to $0.5 < A < 1$ (see the shape of the refractive surface corresponding to Fig. 18c) and to a density through. The behaviour of the ray path is however different in the two cases. In the case of the crest

5

with $\Lambda \neq 0$ (Fig. 30a), the ray angle, as we have seen, has the same sign and rotates in the same direction as the wave normal. Thus, the ray path lies on the same side of the wave normal. In the case of the density through and with $0.5 < \Lambda < 1.0$, due to the different shape of the refractive index surface, the ray moves initially to the left (R_0) when the initial wave normal is to the right and continues to move in a sense opposite to that of the wave normal, which means that it rotates away from regions of increasing refractive index (i.e. increasing density). It follows that trapping at frequencies $> 0.5 \omega_{pe}$ can occur only in density troughs (and not in crests).

What is important to derive now is the value of ionization density variation necessary to trap the ray in the slab. If we denote with $N(0)$ the electron density on the axis of the irregularity and with $N(P)$ the density value at the outermost excursion of the ray path from the axis, there is clearly a relation between the initial wave normal angle θ_0 and the initial density ratio $N(P)/N(0)$ required for trapping or, viceversa, for a given density ratio, there is a critical angle for trapping. To derive this, we have simply to note that, in both cases of Figs. 30a and b, the wave normal direction becomes parallel to H_0 at the maximum ray path excursion. Then, applying Snell's law we obtain

$$\mu[N(0), \theta_0] \cos \theta_0 = \mu[N(P), 0] \quad (6.4)$$

from which, using the expression (6.1) for the refractive index, we arrive at

$$\frac{N(P)}{N(0)} = \frac{1 - \Lambda}{\omega^2 \theta_0 - \Lambda} \omega^2 \theta_0 \quad (6.5)$$

For $\Lambda \neq 0$, eq. (6.5) gives more simply the relation

6

$$\frac{N(P)}{N(0)} \sim \omega^2 \theta_0 \quad (6.6)$$

6.3.2. Case $0 < \Lambda < 0.5$

The conditions for trapping when $0 < \Lambda < 0.5$ must be deduced separately owing to the different features of the refractive index surfaces (see Fig. 18b) and can be derived from figures 32a and b (taken from Helliwell, 1965). We have already introduced the angle $\theta_2 = \arccos 2\Lambda$ (see 6.3) such that, at $\theta = \pm \theta_2$, the ray direction becomes parallel to the magnetic field.

For initial wave normal angles

$$0 < \theta_0 < \theta_2 \quad (6.7)$$

the refractive index surface (as seen from Fig. 32a) has the same shape of the surface corresponding to $\Lambda \neq 0$. Hence, for the case of a crest irregularity, as we already saw, trapping will be possible for such initial angles and the fractional density gradient required for trapping is that given by eq. (6.5). Furthermore, the maximum excursion of the ray occurs when the wave normal angle becomes $\theta = \theta_2$.

Let us now see what is the ray path and the trapping condition for a through irregularity. A third angle θ_3 , indicated in Fig. 32a can be now defined (and can be only for $0 < \Lambda < 0.5$ and a through) as that angle at which the projection of the refractive index vector on the H_0 axis is equal to $\mu(0)$, i.e.

$$\mu(\theta_3) \cos \theta_3 = \mu_0 \quad (6.8)$$

7

from which we obtain

$$\omega \theta_3 = \frac{\lambda}{1 - \lambda} \quad (6.9)$$

Then, a ray starting with $\theta_0 = \theta_3$ at $y=0$ (point of maximum depression) would initially bend towards the axis (and so does the wave normal). When the wave normal angle reaches the value θ_2 , given by (6.3), the ray becomes parallel to H_0 and, again, we have maximum lateral excursion. Then the ray starts bending on the opposite side and the final ray trajectory is of the type shown in Fig. 31c. This type of ray path actually occurs for all initial angles

$$0 < \theta_0 < \theta_3 \quad (6.10)$$

If the initial angle θ_0 becomes greater than θ_3 and, more precisely, if

$$\theta_3 < \theta_0 < \theta_L \quad (6.11)$$

where θ_L (see the asymptote in Fig. 32a) is defined as the limiting angle for wave propagation (see eq. 6.2), i.e. $\theta_L = \arccos \lambda$, the behaviour of ray trapping in the through is still different.

Let us follow the sequence of ray directions, starting with the initial direction R_0 , through Fig. 32b. The direction R_0 is away from the axis of the duct; it implies a lateral displacement towards an increased value of density (refractive index μ_1). The normal to H_0 from the origin of R_0 intersects μ_1 and so the new direction R_1 is found which is less inclined with respect to H_0 than R_0 but still implies more lateral displacement. We then find the crossing with the curve μ_2 corresponding to a furtherly increased value of density and there we find the new ray direction R_2 , even less inclined with respect to H_0 . In

8

this way, the wave normal angle (which also has decreased from its initial value θ_0) reaches the value θ_2 at which the ray becomes parallel to H_0 and then starts bending towards the axis of the duct. This implies now a lateral displacement towards the center (decreasing density). The normal to H_0 from the origin of R_2 intersects the μ_2 surface at a certain point wherein we find a new direction of the ray R_3 which is now bent towards the axis of the irregularity. It is the direction which the ray has when, having passed the value θ_2 of wave normal, it reaches again the density corresponding to μ_2 . From now on we move towards decreasing density. Hence, from the origin of R_3 on the curve μ_2 we must intersect μ_1 (the next value of decreased density). This gives the new ray direction R_4 which is still bent towards the axis of the duct but less inclined than R_3 with respect to H_0 . When it reaches $\theta=0$, the ray is again parallel to H_0 and then starts bending away, i.e. goes towards regions of increasing density. The line from the origin of R_4 (on μ_1) still intersects of μ_1 surface at a second point where we get the new ray direction R_5 . From here we have to move to higher density values. Thus we intersect first μ_2 on the left side of Fig. 32b (wave normal angle negative) reaching the direction R_6 . In the meantime the wave normal angle is approaching the value $\theta = -\theta_2$ where the ray becomes again parallel to the y axis to start bending afterwards towards the axis again (increasing density). The normal to H_0 at the origin of R_6 (on μ_2) intersects μ_2 again at the point where we get R_7 . From here, as the density increases, we must cross μ_1 where we get R_8 (more inclined than R_7 with respect to H_0). When the wave normal reaches the value $-\theta_3$ (defined in (6.9)), the direction is R_9 and we are back again at the surface μ_0 , i.e. the ray is crossing, with maximum inclination, the duct axis. Then the ray path repeats itself on the right hand side of the irregularity. Its shape is that given in Fig. 31b.

Finally, let us derive the fractional density gradient required for trapping in a through, for $0 < \Lambda < 0.5$ and both the cases $0 < \theta < \theta_3$ and $\theta_3 < \theta < \theta_L$ described before. As in both cases the maximum lateral extent of the ray is found at $\theta = \theta_2 = \arccos 2\Lambda$, from the usual Snell's law we obtain (θ_0 being the initial angle at $y=0$)

$$\left[\frac{N(0)}{\Lambda(\omega\theta_0 - \Lambda)} \right]^{1/2} \frac{\omega\theta_0}{\omega_{Be}} = \left[\frac{N(P)}{\Lambda^2} \right]^{1/2} \frac{2\Lambda}{\omega_{Be}}$$

from which

$$\frac{N(P)}{N(0)} = \frac{\omega^2 \theta_0}{4\Lambda(\omega\theta_0 - \Lambda)} \quad (6.12)$$

6.3.3 Summary of the ray theory of trapping of whistlers in ducts

Let us summarize what we have found separating, this time, the cases of a crest and that of a through irregularity.

For a crest, trapping has been found possible only for frequencies

$$0 < \Lambda < 0.5 \quad (6.13)$$

but not for frequencies above $\Lambda=0.5$. This is in agreement with the observational evidence (Smith, 1960) that, for all nose whistlers there is a cutoff frequency whose ratio to the established minimum gyrofrequency along the path never exceeds $\Lambda \sim 0.5 \pm 0.6$. The typical ray path for

trapping in a crest, and the frequency range (6.13) is that shown in Fig. 31a. The critical fractional density gradient required for trapping is given, in terms of the wave normal angle θ_0 at the axis of the crest, by

$$\frac{N(P)}{N(0)} = \frac{1 - \Lambda}{\omega\theta_0 - \Lambda} \omega^2 \theta_0 \quad (6.14)$$

which, for $\Lambda \sim 0$, reduces to

$$\frac{N(P)}{N(0)} \sim \omega^2 \theta_0 \quad (6.15)$$

Trapping occurs (under the appropriate density gradient) for all values of θ_0 in the range

$$0 < \theta_0 < \theta_2 \quad (6.16)$$

with

$$\theta_2 = \arccos 2\Lambda \quad (6.17)$$

In the case of a through irregularity, trapping can occur for all values of Λ from 0 to 1. When

$$0 < \Lambda < 0.5$$

trapping occurs for all values of θ_0 from zero up to the limiting value for propagation

$$0 < \theta_0 < \theta_L \quad (6.18)$$

with

$$\theta_L = \arccos \Lambda \quad (6.19)$$

As for the ray trajectory, it is of the type sketched in Fig. 31a when $0 < \theta_0 < \theta_2$; it is of the type sketched in Fig. 31c when $\theta_2 < \theta_0 < \theta_3$ and of the type seen in Fig. 31b when $\theta_3 < \theta_0 < \theta_L$, the angle θ_3 being defined as

$$\theta_3 = \arccos \frac{\Lambda}{1 - \Lambda} \quad (6.20)$$

In all cases, the critical ionization density gradient is given, in terms of θ_0 by

$$\frac{N(P)}{N(0)} = \frac{\omega^2 \theta_0}{4\Lambda(\omega \theta_0 - \Lambda)} \quad (6.21)$$

Finally, when

$$0.5 < \Lambda < 1 \quad (6.22)$$

trapping is still possible in a through (not in a crest) for all values of θ_0 for which propagation is possible. The trapping condition is given by eq. (6.14) and the ray trajectory is of the type shown in Fig. 31a.

It is convenient to define as enhancement (or reduction) factors the quantities

$$E_c = \frac{N(0)}{N(P)} - 1 \quad (\text{for a crest}) \quad (6.23)$$

$$E_t = \frac{N(P)}{N(0)} - 1 \quad (\text{for a through}) \quad (6.24)$$

O being the axis of the irregularity and P corresponding to the maximum lateral displacement of the ray path. Then, from the trapping condition derived, one obtains the curves of minimum E_c and E_t , reported in Fig. 33 (from Helliwell, 1965) in a plane containing wave normal direction and normalized frequency of the waves.

6.3.4 Some other consequences of the ray theory of whistler trapping in ducts

It is important to consider the effect of a duct on the average group ray velocity. The wave normal of a ducted signal changes periodically direction as the ray path goes back and forth across the duct. The maximum angle with B_0 occurs when the ray crosses the axis of the duct and the corresponding longitudinal component of the ray velocity is correspondingly reduced by the cosine of the angle between the ray and B_0 . At maximum excursion the wave normal angle is zero, but, referring to a crest, the density is reduced, so that the group ray velocity in fact exceeds its value on the axis. It was found (Smith et al., 1960; Smith, 1961) that these factors compensate to give an average group velocity of the ducted wave very nearly (within 1%) the same as that of a strictly longitudinal wave travelling along the axis of the duct. This result is obviously of importance when calculating group delay to compare with whistler's recordings.

Another consequence of the theory of propagation in ducts is that the enhancement required for trapping increases markedly towards the equator, thus providing an explanation for reduced whistler occurrence at low latitudes (Smith et al., 1960). This is easily understood on the basis of the fact that, as whistler waves enter the ionosphere, their wave normals are refracted to the vertical because of the high refractive index. Thus the angle between the earth's field B_0 and the

73

wave normal will increase towards the equator because of the decrease in the dip of magnetic field. As a consequence, one expects trapping to be more difficult towards the equator. This is seen more quantitatively by expressing the wave normal angle θ_0 , which is the complement of the magnetic dip as a function of geomagnetic latitude λ as

$$\tan \theta_0 = \frac{1}{2} \cot \lambda \quad (6.25)$$

If we now suppose that ducting starts in the lower regions of the path where $\lambda \ll 1$, we can use eq. (6.15) for the critical enhancement for trapping in a crest and thus derive, in combination with (6.25), the enhancement factor as a function of geomagnetic latitude. Fig. 34 (from Smith et al., 1960) shows the above mentioned effect which, as already said, is in good agreement with observations.

FIG 30

14

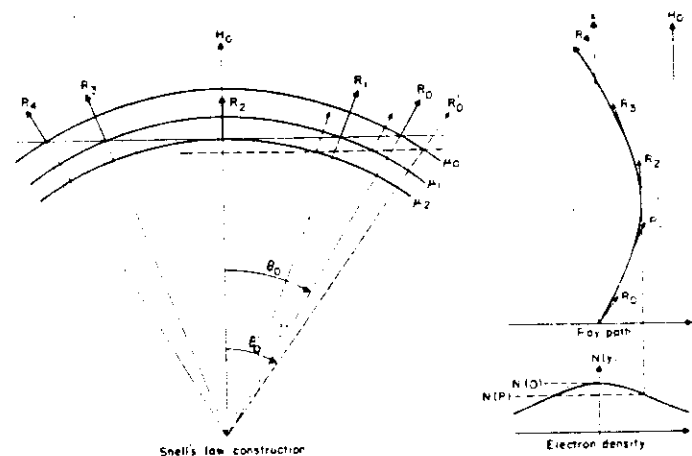
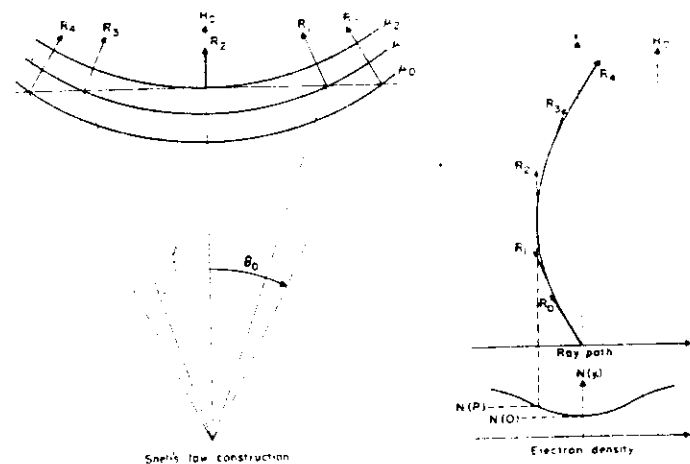
 $\lambda \rightarrow 0$  $0.5 < \lambda < 1$

FIG 31 15

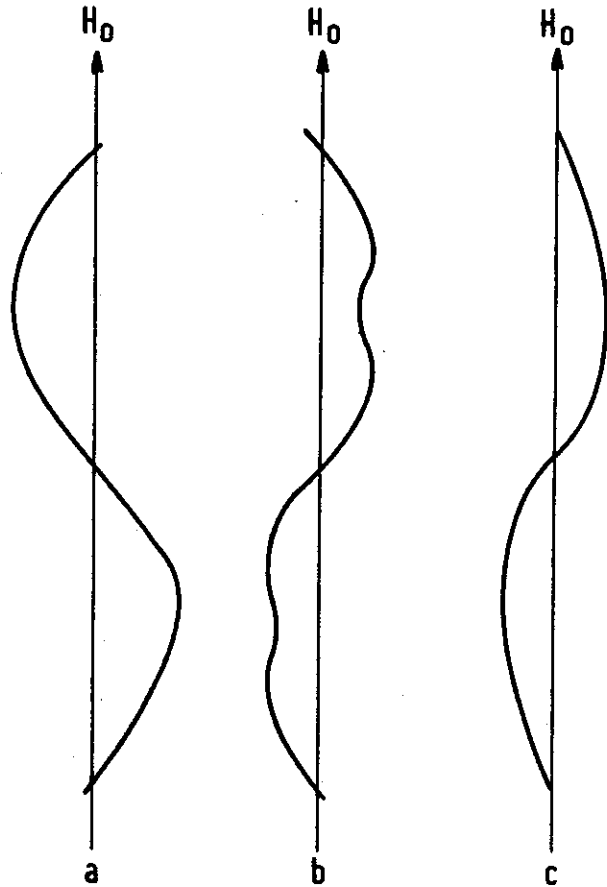
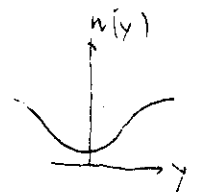
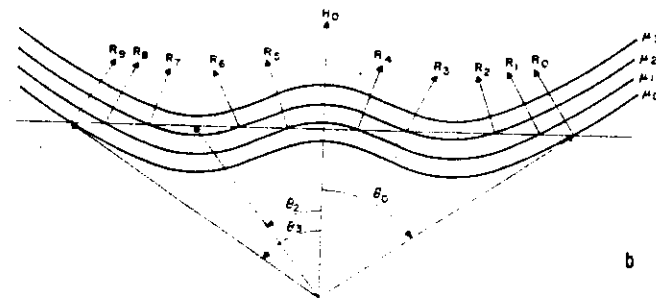
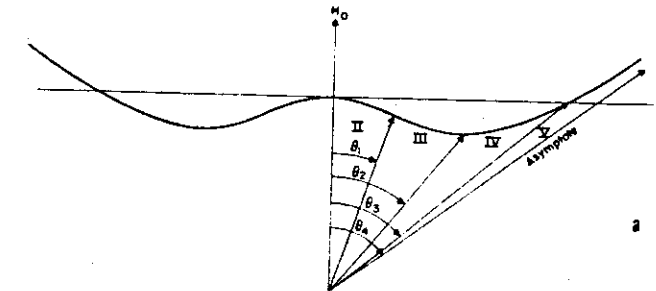


FIG 32 16

$$0 < \Lambda < 0.5$$

- a) $0 < \theta < \theta_2$ west $\frac{N(\theta)}{N(0)} < \cos \theta_0$
 b) $0 < \theta < \theta_3$
 c) $\theta_3 < \theta < \theta_L$



$$\theta_L = \arccos \Lambda$$

$$\theta_2 = \arccos 2\Lambda$$

$$n(\theta_3) \cos \theta_3 = n(0) \rightarrow \cos \theta_3 = \frac{\Lambda}{1-\Lambda}$$

FIG 33 17

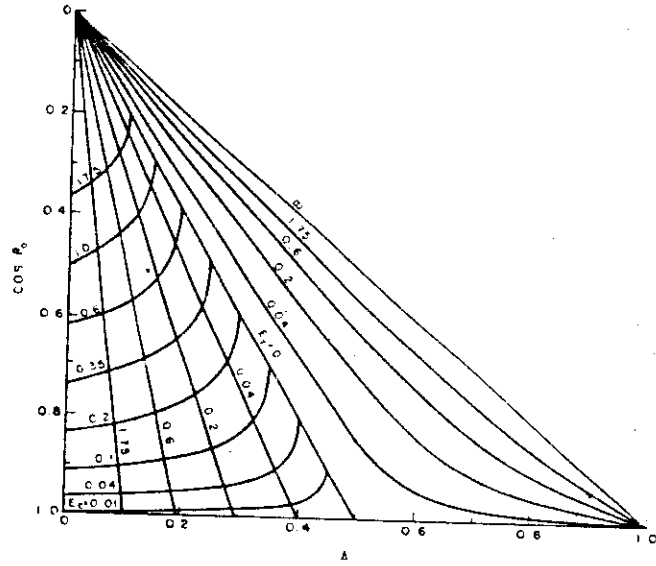


FIG. 34

